

Electron-hole coherence in core-shell nanowires with partial proximity-induced superconductivityKristjan Ottar Klausen ¹, Anna Sitek ², Sigurdur I. Erlingsson ¹ and Andrei Manolescu ¹¹*Department of Engineering, Reykjavik University, Menntavegur 1, IS-101 Reykjavik, Iceland*²*Department of Theoretical Physics, Wrocław University of Science and Technology, Wybrzeże Wyspiańskiego 27, 50-370 Wrocław, Poland*

(Received 8 July 2022; revised 5 January 2023; accepted 9 January 2023; published 23 January 2023)

By solving the Bogoliubov–de Gennes Hamiltonian, the electron-hole coherence within a partially proximitized n -doped semiconductor shell of a core-shell nanowire heterostructure is investigated numerically and compared with the Andreev reflection interpretation of proximity induced superconductivity. Partial proximitization is considered to quantify the effects of a reduced coherence length. Three cases of partial proximitization of the shell are explored: radial, angular, and longitudinal. For the radial case, it is found that the boundary conditions impose localization probability maxima in the center of the shell in spite of off-center radial proximitization. The induced superconductivity gap is calculated as a function of the ratio between the proximitized shell thickness and the total shell thickness. In the angular case, the lowest-energy state of a hexagonal wire with a single proximitized side is found to display the essence of Andreev reflection, only by lengthwise summation of the localization probability. In the longitudinal case, a clear correspondence with Andreev reflection is seen in the localization probability as a function of length along a half-proximitized wire. The effect of an external magnetic field oriented along the wire is explored.

DOI: [10.1103/PhysRevB.107.035423](https://doi.org/10.1103/PhysRevB.107.035423)**I. INTRODUCTION**

Semiconductor nanowires with proximity induced superconductivity have emerged as key elements in various platforms proposed to realize qubits and other emerging technologies at the quantum scale [1–3]. The proximity effect is generally hypothesized to stem from electron-hole coherence, brought on by Andreev reflection at the superconductor interface, where an incoming electron is retroreflected as a hole [4–6]. The superconducting proximity effect has resurfaced time after time in the past decades as a hot research topic due to relevance to research topics in each decade [7–16], most recently due to the search for Majorana zero modes in nanostructures [17–19]. These zero modes are expected to be hosted in synthetic topological superconductors, where p -wave superconductivity can be engineered using spin-orbit coupling in conjunction with Zeeman splitting and proximity induced superconductivity in semiconductors [20–22].

Core-shell nanowires are radial heterojunctions consisting of a core which is wrapped by one or more layers of different materials. Due to crystallographic structure they usually have polygonal cross sections [23–37], and thus the shells become prismatic nanotubes, but circular systems have also been obtained [38]. The sharp corners of the cross section induce nonuniform electron localization along the circumference of the tube, in particular, low-energy electrons are accumulated in the vicinity of sharp edges, while carriers of higher energy are shifted to the facets [39–42]. If the shell is very thin then the low-energy electrons are depleted from the facets and the shell becomes a multiple-channel system consisting of well-separated one-dimensional (1D) electron channels situated along the edges. Due to their unique localization and a

variety of other interesting properties, core-shell nanowires have been extensively investigated in the past two decades [43,44], showing promise in multiple applications such as lasers [45], energy harvesting devices [46,47], and photovoltaics [48]. By n doping, the chemical potential can be moved into the conduction band such that electrons become the only charge carriers and the material behaves effectively as a metal with the effective mass of the host semiconductor. Earlier investigations have indicated that due to 1D electron channels along the sharp edges of prismatic tubes, multiple Majorana zero modes can be hosted in a single core-shell nanowire [49,50]. However, only if the electron-hole coherence length is larger than the whole structure can the shell be considered fully proximitized and electron-hole coherence can be expected to be uniform.

In this paper, electron-hole coherence is investigated in an n -doped semiconductor core-shell nanowire with partial proximity induced superconductivity. Electron-hole coherence of the lowest-energy states is compared with the Andreev reflection picture of proximitized superconductivity in the radial, angular, and longitudinal interfaces arising within a single nanowire.

II. ELECTRON-HOLE COHERENCE AND THE PROXIMITY EFFECT

One of the earlier theoretical descriptions of the spatial dependence of the order parameter in the superconducting proximity effect was done by McMillan [51], using a Green's function approach based on the Gor'kov equations [52] to describe a normal metal-superconductor (NS) junction. In this method, the BCS potential for a quasi-1D problem is written

in terms of the pairing interaction $V(\mathbf{x})$ and the condensation amplitude [11] $F(\mathbf{x})$,

$$\Delta(\mathbf{x}) = V(\mathbf{x})F(\mathbf{x}), \quad (1)$$

where the ensemble average of field operators with opposite spin projections describes the condensation amplitude [53]

$$F(\mathbf{x}) = \langle \hat{\psi}_\uparrow(\mathbf{x})\hat{\psi}_\downarrow(\mathbf{x}) \rangle. \quad (2)$$

McMillan [51] called the problem of the NS junction possibly the simplest one in space-dependent superconductivity and proposed, in his own words, “a very nearly complete solution” of the problem for the case of infinite length of both metals, evaluating

$$F(\mathbf{x}) = \frac{1}{\pi} \int_0^{E_{c_0}} \text{Im}[\mathcal{G}_{12}(E, \mathbf{x}, \mathbf{x}')] dE, \quad (3)$$

where E_{c_0} is the cutoff energy [54]. \mathcal{G}_{12} is the upper off-diagonal component of the 2×2 Green's function

$$\mathcal{G}(\mathbf{x}, t, \mathbf{x}', t') = -i\langle 0|T\{\Psi(\mathbf{x}, t)\Psi^\dagger(\mathbf{x}', t')\}|0\rangle, \quad (4)$$

written in the Nambu [55] spinor formalism,

$$\Psi(\mathbf{x}) = \begin{pmatrix} \hat{\psi}_\uparrow(\mathbf{x}) \\ \hat{\psi}_\downarrow^\dagger(\mathbf{x}) \end{pmatrix}, \quad (5)$$

where T denotes time ordering and $|0\rangle$ the Heisenberg ground state. $F(\mathbf{x})$ is also known as the anomalous Green's function [56].

Another fundamental reference in the field is a book chapter written by Deutscher and de Gennes [57] where the distinction between a clean and dirty junction is made and the following simplified result presented for the spatial dependence of $F(\mathbf{x})$. For a clean metal, where the mean free path l_N therein is larger compared to the coherence length, $l_N > \xi_N$, the asymptotic form is obtained:

$$F(\mathbf{x}) = \phi(\mathbf{x}) \exp\left(-\frac{2\pi k_B T}{\hbar v_F} |\mathbf{x}|\right), \quad (6)$$

where $\phi(\mathbf{x})$ is some slowly varying function, k_B is the Boltzmann constant, T denotes temperature, and v_F is the Fermi velocity. For the limiting case of the temperature being close to zero a result by Falk [58] is cited,

$$F(\mathbf{x}) \sim \frac{1}{|\mathbf{x}|}. \quad (7)$$

Falks paper [58] has a similar Green's function based approach to the Gor'kov equations as McMillan [51] and proceeds McMillan's work by five years. Andreev [4] considered the equations of motion obeyed by components of the Green's function in Eq. (4) in which diagonal and off diagonals are coupled to derive a curious scattering process at the plane boundary between the normal and superconducting phases which now bears his name. Andreev reflection, Fig. 1, is the conjugate retroreflection of electrons and holes at a metal-superconductor boundary [4]. Retroreflection means that an incoming electron from the normal metal side is reflected such that it traces back the incident trajectory. In order for an incident electron at the normal metal side with energy below the gap parameter Δ to be transferred across the boundary, the formation of a Cooper pair in the superconductor

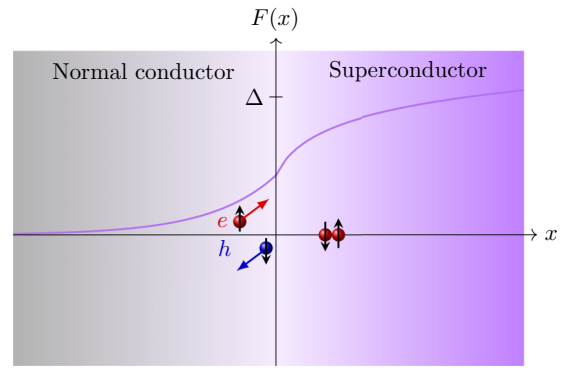


FIG. 1. Simplified sketch of the proximity effect in terms of the condensation amplitude $F(x)$ and Andreev reflection. An electron with energy $E < \Delta$ at an N-S boundary will be *retroreflected* as a hole while forming a Cooper pair within the superconductor [6].

requires another electron with equal and opposite momentum, which can be seen as a reflected hole.

At present time, electron-hole coherence via Andreev reflection is considered to be the mechanism behind the superconducting proximity effect [59,60]. Blonder, Tinkham, and Klapwijk (BTK) refined the scattering approach to the problem using the Bogoliubov equations and further computed I - V curves along with transmission and reflection coefficients for all cases of energy relative to the superconducting gap including a delta barrier at the interface [6]. This work has since become seminal for Andreev reflection and is fundamental to most tunneling spectroscopy experiments on superconducting junctions [59]. The scattering formalism has the advantage of being readily interpreted and familiar from the standard educational problem in quantum mechanics of scattering from a potential barrier. Klapwijk [11] later noted that the following self-consistency equation was not incorporated in the original BTK approach and the superconducting gap implemented as a step function at the interface. The self-consistency equation can be written as

$$\Delta(\mathbf{r}) = V(\mathbf{r})F(\mathbf{r}) = V(\mathbf{r}) \sum_E u(\mathbf{r})v^\dagger(\mathbf{r})[1 - 2f(E)], \quad (8)$$

where $u(\mathbf{r})$ and $v(\mathbf{r})$ are the electron and hole components of the quasiparticle wave function, respectively, and $f(E)$ is the Fermi-distribution function,

$$f(E) = \{1 + \exp[E - \mu/(k_B T)]\}^{-1}. \quad (9)$$

Even if the pairing interaction $V(\mathbf{r})$ is zero in the normal metal, $F(\mathbf{r})$ can be nonzero, stemming from electron-hole coherence, which can be interpreted as the superconductivity leakage in the normal metal [11]. The self-consistency equation determines the variation of $\Delta(\mathbf{r})$ at the intersection but the general features of Andreev reflection are independent of it [61]. Self-consistency has been shown to be of great importance for interfaces with d -wave superconductivity [62,63]. The spatial propagation of the superconducting order parameter at NS interfaces has been found [64] to be adequately described by the Usadel equations [65], which are a diffusive (dirty) limit of the Eilenberger-Larkin-Ovchinnikov equations [66,67], which are a quasiclassical approximation to the Gorkov equations [52]. The Gorkov equations can be

used to derive the semiclassical Ginzburg-Landau theory [68] from a microscopic description [69].

Considerable work has been done in the past decade on the many subtleties of the superconducting gap parameter in hybrid semiconductor-superconductor systems in relation to the quest for experimental realization of Majorana zero modes [70–74], in particular, where p -wave superconductivity is engineered in nanowires by combining the proximity effect and Zeeman and Rashba spin-orbit interaction [21]. Another promising approach are hybrid systems using ferromagnetic materials [75] to obtain spin-triplet pairing [76–81] allowing for topological states [82]. Properties of the induced gap can be significantly altered in the presence of ferromagnetism [83–87]. Furthermore, interfaces of superconductors and ferromagnetic materials have opened up possibilities for superconducting spintronics [88,89], allowing for spin-dependent control of supercurrents [90,91] and transition temperatures [92,93].

III. MODEL AND METHODS

A three-dimensional proximitized core-shell nanowire is modeled in the zero temperature limit using cylindrical coordinates, where the z axis is defined along the wire growth direction. Using a divide and conquer algorithm [94] coded in FORTRAN [95], energy spectra and states of the system are obtained by numerical diagonalization of the Bogoliubov–de Gennes (BdG) Hamiltonian [96,97],

$$H_{\text{BdG}} = \begin{pmatrix} [H_w - \mu] & \pm \Delta_{\uparrow\downarrow} \\ \mp \Delta_{\uparrow\downarrow}^* & -[H_w^* - \mu] \end{pmatrix}. \quad (10)$$

The matrix elements are written in the composite basis $|q\rangle$ consisting of the transverse modes $|a\rangle$, longitudinal modes $|n\rangle$, spin $|\sigma\rangle$, and particle-hole eigenstates $|\eta\rangle$, such that

$$|q\rangle = |\eta a n \sigma\rangle, \quad (11)$$

where $|a n \sigma\rangle$ are the eigenstates of the Hamiltonian for the wire without proximity induced superconductivity,

$$H_w = H_t + H_l + H_z. \quad (12)$$

The transverse and longitudinal components of the Hamiltonian are written as

$$H_t + H_l = \frac{(p_\phi + eA_\phi)^2}{2m_e} - \frac{\hbar^2}{2m_e r} \frac{\partial}{\partial r} \left(r \frac{\partial}{\partial r} \right) + \frac{p_z^2}{2m_e}, \quad (13)$$

where $A_\phi = \frac{1}{2} B r$ is the vector potential in the symmetric gauge, incorporating an external magnetic field, \mathbf{B} , directed along the wire axis. The transverse eigenstates are expanded in terms of the lattice sites

$$|a\rangle = \sum_{\kappa} c_a |r_\kappa \phi_\kappa\rangle \quad (14)$$

and matrix elements obtained by finite-difference discretization of derivatives [41,42]. The cross-section geometry is added by infinite potential boundary conditions defining the hexagonal shape. For an infinite wire, the longitudinal modes are expressed in an exponential plane wave basis so that the Hamiltonian becomes a function of the longitudinal wave vector. For a finite wire, they are expanded in a sine

basis,

$$|n\rangle = L_z^{-1/2} \sqrt{2} \sin \left[n\pi \left(\frac{z}{L_z} + \frac{1}{2} \right) \right]. \quad (15)$$

The length of the wire is L_z ; the origin is defined in the nanowire center so that the wire spans the interval $[-\frac{L_z}{2}, \frac{L_z}{2}]$ along the z axis. The external magnetic field B gives rise to the Zeeman term

$$H_z = -g^* \mu_B \sigma B, \quad (16)$$

where g^* is the effective Landé g factor and μ_B the Bohr magneton. The particle-hole symmetry and coupling are contained in the quantum number $\eta = \pm 1$ and the matrix elements of the BdG Hamiltonian are obtained by the following, for $\eta = \eta'$,

$$\begin{aligned} \langle a n \sigma \eta | H_{\text{BdG}} | a' n' \sigma' \eta' \rangle \\ = \eta [\text{Re} \langle a n \sigma | H_w | a' n' \sigma' \rangle \\ + i \eta \langle a n \sigma | H_w | a' n' \sigma' \rangle - \mu \delta_{(a n \sigma)(a' n' \sigma')}], \end{aligned} \quad (17)$$

and for $\eta \neq \eta'$,

$$\langle a n \sigma \eta | H_{\text{BdG}} | a' n' \sigma' \eta' \rangle = \eta \sigma \delta_{\sigma, -\sigma'} \delta_{a a'} \delta_{n n'} \Delta_s. \quad (18)$$

The chemical potential, μ , is set to correspond to an n -doped semiconductor such that electrons are the main carriers of the system. In accordance with the original works of Andreev [4] and BTK [6], the induced gap is a fixed parameter and spin-orbit coupling is not considered. Partial proximitization is implemented in the superconducting gap parameter, $\Delta_s(r, \phi, z)$, by step functions of position in the radial, angular, and longitudinal direction of the shell, so that ideal junctions with no interface barriers [98] are formed in each case. No further boundary condition is imposed at the interface apart from the step function of Δ_s , which is known as a rigid boundary condition [99]. Model parameters are set to correspond to an InSb shell with $\gamma = \frac{1}{2} g^* m_e = 0.393$ and $\Delta = 0.50$ meV. The numerical simulations were performed for single shell nanowires with cross-section diameter of 100 nm and shell thickness $d = 10$ nm, the length was set to 10 μm in Secs. IV and V along with a shorter wire of 1 μm , and an infinite one explored in Secs. VI and IV, respectively.

IV. PARTIAL RADIAL PROXIMITIZATION

A core-shell nanowire fully coated with a superconducting layer has a radially symmetric proximity induced gap in the shell. Full-shell nanowire systems allow for additional control of the superconducting energy gap due to the Little-Parks effect [100–102]. Multiple fabrication-specific microscopic details and material properties can influence the strength of the induced gap [103]. To investigate electron-hole coherence within the partially proximitized shell, the semiconductor shell is considered to have a superconducting gap Δ_s in its outer half, brought on by a surrounding superconductor, not included in the Hamiltonian. A cylindrical shell is studied to isolate the effect of a partial proximitization radially, Fig. 2(a). As the interface lies within the semiconductor shell, there is no Fermi surface mismatch. Partial proximitization of a semiconductor wire with a superconductor having a gap $\Delta_s = 0.5$ meV results in an induced gap of $\Delta_i = 0.15$ meV of the whole system, Figs. 2(b) and 2(c). The wave function acquires

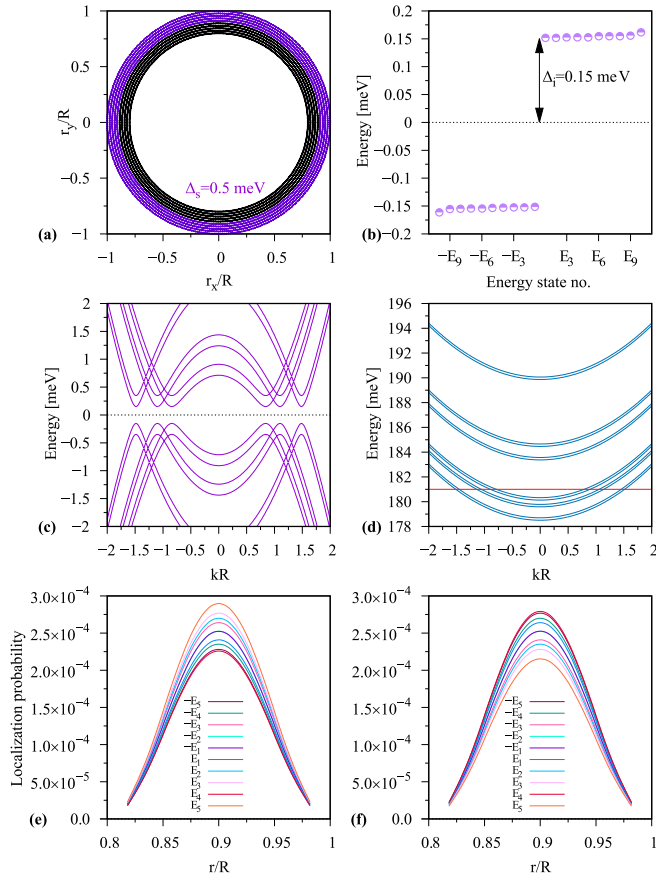


FIG. 2. (a) Partial radial proximitization of the nanowire shell, diameter of $2R$. Half-proximitized shell with $\Delta_s = 0.5$ meV in the outer half (purple) of the shell. (b) Finite wire BdG spectrum of the nanowire system, showing the induced gap $\Delta_i = 0.15$ meV. (c) Infinite wire BdG energy dispersion in terms of the dimensionless product of the wave vector, k , and radius, R . (d) Energy dispersion and chemical potential (red) of the infinite wire. (e) Longitudinal summation of localization probability on interior sites for the hole component $|v|^2$ of the lowest positive and negative energy states, for a single angular slice. (f) Corresponding electronic component $|u|^2$.

the angular symmetry of the shell; the localization probability peak, however, is found to be centralized in the shell, irrespective of the radial asymmetry of proximitization. This follows from the boundary condition of no hopping over the inner and outer boundary of the shell, which corresponds to vanishing of the wave function in the continuous lattice limit. Note that, according to Eq. (15), the localization probability oscillates along the wire length. The oscillation wavelength is determined by the chemical potential, Fig. 2(d), as the higher energy level increases the frequency. Figures 2(e) and 2(f) show the longitudinal summation of localization probability for the first five positive and negative energy states. The boundary conditions force the induced hole component to be equally localized over both the proximitized and non-proximitized parts of the wire shell. In this case, finite size effects [98,104] dominate over scattering, leading to a uniform electron-hole coherence and an induced gap in the whole shell. In Fig. 3 the induced superconducting gap is shown as a function of the ratio between the nonproximitized and

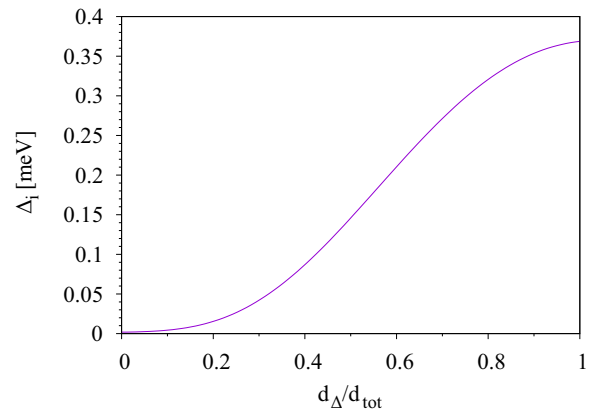


FIG. 3. Induced superconducting energy gap of a partially proximitized nanowire as a function of the ratio of the proximitized shell thickness, d_Δ , to the total shell thickness, d_{tot} .

proximitized parts of the shell. The results are found to be independent of the shell thickness, for the given diameter of the wire. The superconducting gap parameter of the proximitized part is set to $\Delta_s = 0.5$ meV. The induced superconducting gap of the fully proximitized system is lowered by 10% due to the applied external magnetic field, $|\vec{B}| = 65.8$ mT, included in the simulation to lift spin degeneracy. The spin degeneracy is lifted to identify the chemical potential range that includes both spins in the presence of a magnetic field, the effects of which are further studied in Sec. VI.

V. PARTIAL ANGULAR PROXIMITIZATION

Systems where nanowires are proximitized by fabrication of the wire on top of a superconducting slab are common experimental platforms for Majorana physics [105–107]. A hexagonal core-shell structure is considered to model such a system where the effective coherence length is smaller than the diameter of the nanowire, such that only a single side can be considered fully proximitized, Fig. 4(a). In the fully proximitized part, the gap parameter is set at $\Delta_s = 1$ meV and the induced gap obtained is $\Delta_i = 0.05$ meV, Figs. 4(b) and 4(c). For the first excited positive energy quasiparticle state, in the case of the chemical potential including only the lowest-energy band, Fig. 4(d), the Andreev picture of the proximity effect is uncovered. However, it is only seen by lengthwise summation of localization probability such that the total localization probability is projected onto the wire cross section, Figs. 4(e) and 4(f). The fully proximitized part of the semiconductor shell has a hole component localized within it, by definition of the BdG quasiparticle spectrum. Reminiscent of Andreev reflection, the hole components spread out to the normal conducting part of the shell, Fig. 4(e). The electron localization probability is lowered within the superconducting shell, Fig. 4(f), in accordance with the view that the superconductor incorporates an electron to form a Cooper pair and reflects a hole in the process [6]. The electron-hole coherence results in a near uniformly spread out BdG localization probability over the shell with peaks in the corners, due to corner localization [41]. The first negative energy state has the opposite electron-hole localization probability from Figs. 4(e) and

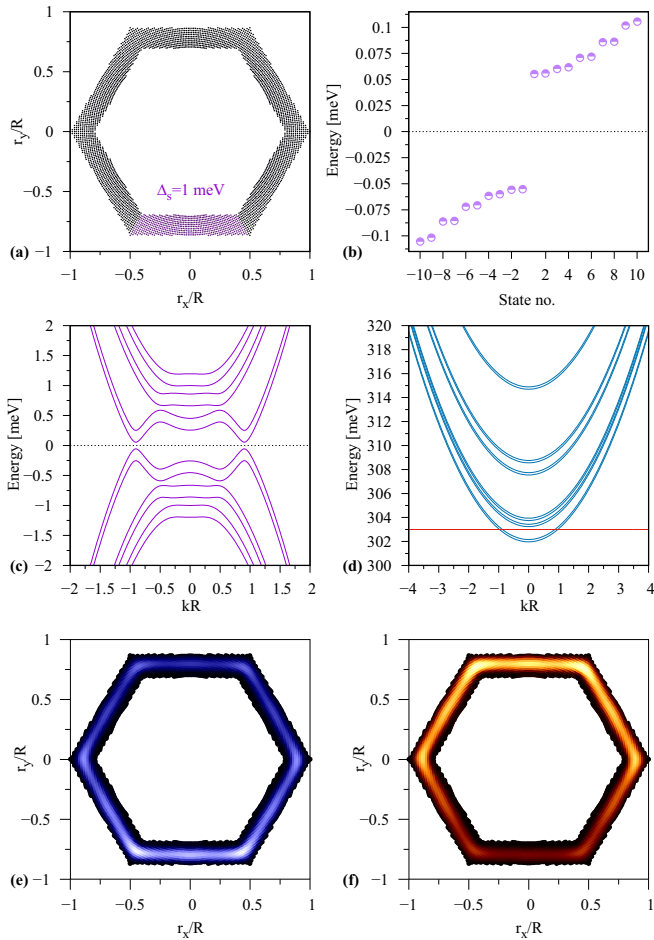


FIG. 4. (a) Partial angular proximitization of a hexagonal nanowire shell; single side proximitization with $\Delta_s = 1$ meV. (b) Finite wire BdG spectrum of the whole system, showing the induced gap $\Delta_i = 0.05$ meV. (c) Infinite wire BdG spectra. (d) Dispersion and chemical potential (red) of the infinite wire Hamiltonian. (e) Longitudinal summation of localization probability for the hole component $|v|^2$ of the lowest positive energy state; brightness denotes higher localization probability. (f) Corresponding electron component $|u|^2$.

4(f), as expected from electron-hole symmetry of the system. Along the length of the wire, the wave function localization probability of each state oscillates, Sec. VI, and the symmetry of Figs. 4(e) and 4(f) can be inverted at specific sites. This also happens for the adjacent higher energy states in which the particle-hole coherence is inverted since for a given energy value of the BdG spectra slightly above Δ , there are four states in each band—two electron dominant and the other two hole dominant.

VI. PARTIAL LONGITUDINAL PROXIMITIZATION

Another possibility of partial proximitization is partial covering of a nanowire longitudinally with a superconductor [105,108]. A half proximitized wire is considered, such that the superconducting gap is uniform in the whole shell up to half the length of the wire, with $\Delta_s = 0.5$ meV. Figure 5 shows the electron-hole coherence at a single corner

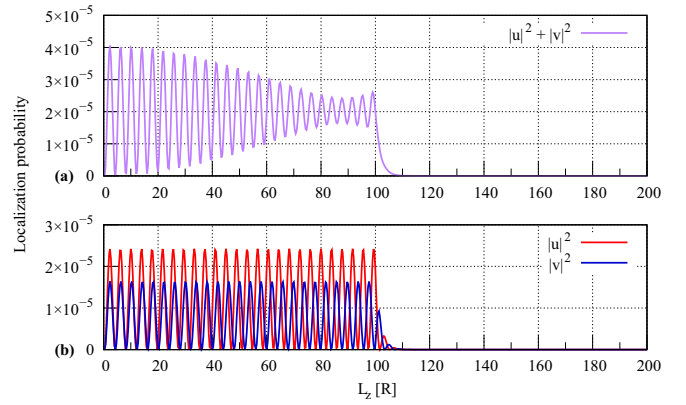


FIG. 5. (a) Single corner site localization probability from the composite BdG wave function of the lowest-energy state of a half proximitized hexagonal wire with no external magnetic field. (b) Corresponding electron and hole components, $|u|^2$ and $|v|^2$, respectively.

site, for the case of no external magnetic field, of a long hexagonal nanowire with $L = 200$ R, where the diameter of the wire is 100 nm. An exponential decay of the composite BdG localization probability into the nonproximitized part is obtained, Fig. 5(a). This stems from coherence of electron and hole tunneling tails into the nonproximitized half of the wire, Fig. 5(b). Diminishing of the BdG localization probability in the proximitized half of the wire is caused by a phase difference between the electron and hole wave function components; the $-\pi/2$ phase difference is characteristic of Andreev reflection [61,109].

If an external magnetic field is applied, Zeeman splitting gives rise to a difference of the k vectors between the spin-split states, resulting in an additional phase difference between the electron and hole components, Fig. 6(b). This phase difference leads to a beating pattern of the BdG localization probability, Fig. 6(a).

In the case of a weaker superconducting gap parameter $\Delta_s = 50$ μ eV, Fig. 7, the exponential decay into the semi-

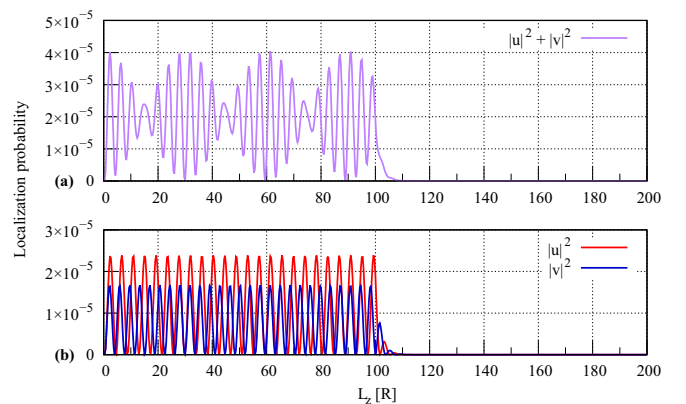


FIG. 6. (a) Single corner site localization probability from the composite BdG wave function of the lowest-energy state of a half proximitized hexagonal wire, for the case of an external magnetic field $|\vec{B}| = 65.8$ mT. (b) Corresponding electron and hole components, $|u|^2$ and $|v|^2$, respectively.

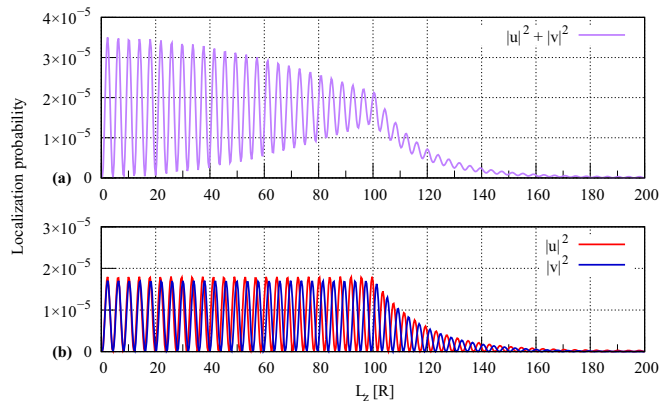


FIG. 7. (a) Single corner site localization probability from the composite BdG wave function of the lowest-energy state of a half proximitized hexagonal wire, $\Delta_S = 50 \mu\text{eV}$, with no external magnetic field. (b) Corresponding electron and hole components, $|u|^2$ and $|v|^2$, respectively.

conducting part is enlarged compared with Fig. 5. The gap parameter can thus be seen as an effective potential barrier for the electron-hole coherence. For a shorter wire with $L = 1 \mu\text{m}$ and $\Delta_S = 0.5 \text{ meV}$, Fig. 8, the exponential decay is less pronounced, compared with Fig. 5. The coherence length is the same but the electron component at the interface is near minimum in phase, rather than at maximum as in the case of the longer wire. The wavelength of the wave function depends on the Fermi level, and so the length can influence the phase value of the electron and hole components at the interface. For both finite wires, long and short, a direct correspondence with Andreev reflection is found per site of the shell, where the propagation of the quasiparticle wave function into the nonproximitized part can be understood in terms of the electron-hole coherence.

VII. DISCUSSION

The manifestation of Andreev reflection in the electron-hole coherence of the lowest-energy quasiparticle states of partially proximitized core-shell nanowires has been investigated by separately considering radial, angular, and longitudinal interfaces of an induced superconducting pairing potential. In the radial case, finite-size effects in the thin shell lead to in-phase electron and hole components, with a symmetric distribution of the total localization probability over the interface. The shell is therefore found to be uniformly gapped, with the superconducting gap of the wire as a whole

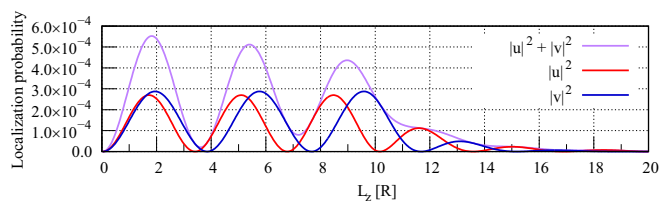


FIG. 8. Single corner site localization probability of the composite BdG wave function and its corresponding electron $|u|^2$ and hole $|v|^2$ components of the lowest positive energy state. Wire length is $L = 1 \mu\text{m}$.

being suppressed with respect to the proximitized gap. For the angular case, asymmetry of the total localization probability over the interface of the lowest-energy state is shown to correspond to Andreev reflection phenomenology. Including higher energy states results in more complex distributions of the total localization probability, worthy of further investigation, as higher order scattering events come into play. The most direct correspondence to Andreev reflection is found for the longitudinal interface, where the electron-hole coherence propagates the quasiparticle wave function into the nonproximitized part of the wire. This is found for each transverse site, which is effectively a one-dimensional nanowire. The results confirm the applicability of the phenomenology for partially proximitized wires of these dimensions. Andreev reflection as described by BTK [6] is a one-dimensional picture of electron-hole coherence from scattering at infinite normal conductor-superconductor (NS) interface, utilizing the Andreev approximation $k_{e/h}^N \approx k_{e/h}^S \approx k_f$, i.e., that all wave vectors are evaluated around the Fermi level. The notion has proven to be very useful for understanding multiple aspects of hybrid superconductor systems in the past decades [5,11] and is still in full use [110,111]. It is, however, an effective single-channel model and limitations of the phenomenology can be expected to come to light with increasing complexity and diversity of fabricated systems [112,113]. Significance of normal reflection events for two-dimensional interfaces has been shown analytically [114,115]. The scattering approach has been shown to have its merits in multiple regimes [116] and even advantages over quasiclassical Green's function approaches [117]. However, incorporating self-energy corrections from the superconductor in the Green's function of proximitized nanowires has been shown to capture important renormalization effects on proximity-induced topological superconductivity [118], and has recently been used to quantify the effects of disorder and Fermi surface mismatch in thin-film proximitization [103]. The current methodology of numerical diagonalization of the system in a position representation is closer to the scattering approach, providing real-space solutions of the wave functions.

VIII. CONCLUSIONS

Low-energy physics of the radial, angular, and longitudinal superconductor interfaces of proximitized core-shell nanowires has been explored using the Bogoliubov-de Gennes equations. Partial proximitization is considered to quantify the effects of a reduced coherence length and to investigate the Andreev reflection interpretation of proximity induced superconductivity. For a thin shell, boundary conditions are found to impose symmetry of the localization probability in spite of partial radial proximitization. In the case of a hexagonal wire with a single proximitized side, it is only by lengthwise summation of localization probability that the essence of Andreev reflection can be seen. For a longitudinally half proximitized wire, electron-hole coherence is explicitly shown to propagate the quasiparticle wave function into the nonproximitized part of the wire. Application of an external magnetic field directed along the wire axis is found to cause amplitude modulation of the quasiparticle wave function. Correspondence with Andreev

reflection is obtained per site of the shell, from considering the localization probability as a function of length in the core-shell nanowire. The results show in what way Andreev reflection is compatible with electron-hole coherence at the various interfaces that can arise in proximitized core-shell nanowire systems.

ACKNOWLEDGMENTS

This research was supported by the Reykjavik University Research Fund, Project No. 218043, and the Icelandic Research Fund, Grant No. 206568-051. We thank T. Schäpers and V. Gudmundsson for discussions.

- [1] M. Hays, V. Fatemi, D. Bouman, J. Cerrillo, S. Diamond, K. Serniak, T. Connolly, P. Krogstrup, J. Nygård, A. L. Yeyati, A. Geresdi, and M. H. Devoret, *Science* **373**, 430 (2021).
- [2] R. Aguado, *Appl. Phys. Lett.* **117**, 240501 (2020).
- [3] M. Benito and G. Burkard, *Appl. Phys. Lett.* **116**, 190502 (2020).
- [4] A. F. Andreev, *Zh. Eksp. Teor. Fiz.* **46**, 1823 (1964) [*JETP* **19**, 1228 (1964)].
- [5] B. Pannetier and H. Courtois, *J. Low Temp. Phys.* **118**, 599 (2000).
- [6] G. E. Blonder, M. Tinkham, and T. M. Klapwijk, *Phys. Rev. B* **25**, 4515 (1982).
- [7] F. Setiawan, C.-T. Wu, and K. Levin, *Phys. Rev. B* **99**, 174511 (2019).
- [8] T. D. Stanescu, R. M. Lutchyn, and S. Das Sarma, *Phys. Rev. B* **90**, 085302 (2014).
- [9] W. A. Muñoz, L. Covaci, and F. M. Peeters, *Phys. Rev. B* **87**, 134509 (2013).
- [10] G.-Q. Zha, L. Covaci, S.-P. Zhou, and F. M. Peeters, *Phys. Rev. B* **82**, 140502(R) (2010).
- [11] T. M. Klapwijk, *J. Supercond.* **17**, 593 (2004).
- [12] A. Jacobs, R. Kümmel, and H. Plehn, *Superlattices Microstruct.* **25**, 669 (1999).
- [13] A. I. D'yachenko and I. V. Kochergin, *J. Low Temp. Phys.* **84**, 197 (1991).
- [14] C. van Haesendonck, L. V. den Dries, Y. Bruynseraede, and A. Gilabert, *J. Phys. F* **11**, 2381 (1981).
- [15] H. Meissner, Semiannual Report No. SIT-P263(10/71), Stevens Institute of Technology, Hoboken, N.J., Department of Physics, Report No. NASA-CR-124627, National Aeronautics and Space Administration, Grant No. NGL-31-003-020 (1971), available at <https://ntrs.nasa.gov/citations/19720004977>.
- [16] J. Clarke, *J. Phys. Colloq.* **29**, C2 (1968).
- [17] E. Prada, P. San-Jose, M. W. A. de Moor, A. Geresdi, E. J. H. Lee, J. Klinovaja, D. Loss, J. Nygård, R. Aguado, and L. P. Kouwenhoven, *Nat. Rev. Phys.* **2**, 575 (2020).
- [18] C. Jünger, A. Baumgartner, R. Delagrèze, D. Chevallier, S. Lehmann, M. Nilsson, K. A. Dick, C. Thelander, and C. Schönenberger, *Commun. Phys.* **2**, 76 (2019).
- [19] R. Aguado, *Riv. Nuovo Cimento* **2017**, 523 (2017).
- [20] T. D. Stanescu, *Introduction to Topological Quantum Matter & Quantum Computation* (CRC Press, London, 2017).
- [21] J. Alicea, *Phys. Rev. B* **81**, 125318 (2010).
- [22] J. D. Sau, R. M. Lutchyn, S. Tewari, and S. Das Sarma, *Phys. Rev. Lett.* **104**, 040502 (2010).
- [23] C. Blömers, T. Rieger, P. Zellekens, F. Haas, M. I. Lepsa, H. Hardtdegen, Ö. Gül, N. Demarina, D. Grützmacher, H. Lüth, and T. Schäpers, *Nanotechnology* **24**, 035203 (2013).
- [24] T. Rieger, M. Luysberg, T. Schäpers, D. Grützmacher, and M. I. Lepsa, *Nano Lett.* **12**, 5559 (2012).
- [25] F. Haas, K. Sladek, A. Winden, M. von der Ahe, T. E. Weirich, T. Rieger, H. Lüth, D. Grützmacher, T. Schäpers, and H. Hardtdegen, *Nanotechnology* **24**, 085603 (2013).
- [26] S. Funk, M. Royo, I. Zardo, D. Rudolph, S. Morkötter, B. Mayer, J. Becker, A. Bechtold, S. Matich, M. Döblinger, M. Bichler, G. Koblmüller, J. J. Finley, A. Bertoni, G. Goldoni, and G. Abstreiter, *Nano Lett.* **13**, 6189 (2013).
- [27] N. Erhard, S. Zenger, S. Morkötter, D. Rudolph, M. Weiss, H. J. Krenner, H. Karl, G. Abstreiter, J. J. Finley, G. Koblmüller, and A. W. Holleitner, *Nano Lett.* **15**, 6869 (2015).
- [28] M. Weiß, J. B. Kinzel, F. J. R. Schüle, M. Heigl, D. Rudolph, S. Morkötter, M. Döblinger, M. Bichler, G. Abstreiter, J. J. Finley, G. Koblmüller, A. Wixforth, and H. J. Krenner, *Nano Lett.* **14**, 2256 (2014).
- [29] J. Jadczyk, P. Plochocka, A. Mitioglu, I. Breslavetz, M. Royo, A. Bertoni, G. Goldoni, T. Smolenski, P. Kossacki, A. Kretinin, H. Shtrikman, and D. K. Maude, *Nano Lett.* **14**, 2807 (2014).
- [30] F. Qian, Y. Li, S. Gradečak, D. Wang, C. J. Barrelet, and C. M. Lieber, *Nano Lett.* **4**, 1975 (2004).
- [31] F. Qian, S. Gradečak, Y. Li, C.-Y. Wen, and C. M. Lieber, *Nano Lett.* **5**, 2287 (2005).
- [32] L. Baird, G. Ang, C. Low, N. Haegel, A. Talin, Q. Li, and G. Wang, *Phys. B: Condens. Matter* **404**, 4933 (2009).
- [33] M. Heurlin, T. Stankevič, S. Mickevičius, S. Yngman, D. Lindgren, A. Mikkelsen, R. Feidenhansl, M. T. Borgström, and L. Samuelson, *Nano Lett.* **15**, 2462 (2015).
- [34] Y. Dong, B. Tian, T. J. Kempa, and C. M. Lieber, *Nano Lett.* **9**, 2183 (2009).
- [35] X. Yuan, P. Caroff, F. Wang, Y. Guo, Y. Wang, H. E. Jackson, L. M. Smith, H. H. Tan, and C. Jagadish, *Adv. Funct. Mater.* **25**, 5300 (2015).
- [36] D. J. O. Göransson, M. Heurlin, B. Dalekhan, S. Abay, M. E. Messing, V. F. Maisi, M. T. Borgström, and H. Q. Xu, *Appl. Phys. Lett.* **114**, 053108 (2019).
- [37] T. Rieger, D. Grützmacher, and M. I. Lepsa, *Nanoscale* **7**, 356 (2015).
- [38] K.-H. Kim and Y.-S. No, *Nano Convergence* **4**, 32 (2017).
- [39] G. Ferrari, G. Goldoni, A. Bertoni, G. Cuoghi, and E. Molinari, *Nano Lett.* **9**, 1631 (2009).
- [40] B. M. Wong, F. Léonard, Q. Li, and G. T. Wang, *Nano Lett.* **11**, 3074 (2011).
- [41] A. Sitek, L. Serra, V. Gudmundsson, and A. Manolescu, *Phys. Rev. B* **91**, 235429 (2015).
- [42] A. Sitek, G. Thorgilsson, V. Gudmundsson, and A. Manolescu, *Nanotechnology* **27**, 225202 (2016).
- [43] M. Royo, M. D. Luca, R. Rurali, and I. Zardo, *J. Phys. D* **50**, 143001 (2017).
- [44] G. Shen and D. Chen, *Nanoscale Res. Lett.* **4**, 779 (2009).
- [45] G. Koblmüller, B. Mayer, T. Stettner, G. Abstreiter, and J. J. Finley, *Semicond. Sci. Technol.* **32**, 053001 (2017).
- [46] C. Florica, A. Costas, N. Preda, M. Beregoi, A. Kuncser, N. Apostol, C. Popa, G. Socol, V. Diculescu, and I. Enculescu, *Sci. Rep.* **9**, 17268 (2019).

- [47] M. A. Hassan, M. A. Johar, A. Waseem, I. V. Bagal, J.-S. Ha, and S.-W. Ryu, *Opt. Express* **27**, A184 (2019).
- [48] S. Z. Oener, S. A. Mann, B. Sciacca, C. Sfiligoj, J. Hoang, and E. C. Garnett, *Appl. Phys. Lett.* **106**, 023501 (2015).
- [49] A. Manolescu, A. Sitek, J. Osca, L. Serra, V. Gudmundsson, and T. D. Stanescu, *Phys. Rev. B* **96**, 125435 (2017).
- [50] K. O. Klausen, A. Sitek, S. I. Erlingsson, and A. Manolescu, *Nanotechnology* **31**, 354001 (2020).
- [51] W. L. McMillan, *Phys. Rev.* **175**, 559 (1968).
- [52] L. P. Gor'kov, *Zh. Eksp. Teor. Fiz.* **34**, 735 (1958) [*JETP* **7**, 505 (1958)].
- [53] A. L. Fetter and J. D. Walecka, *Quantum Theory of Many-Particle Systems* (Dover, New York, 2003).
- [54] X. H. Zheng and D. G. Walmsley, *Phys. Rev. B* **71**, 134512 (2005).
- [55] Y. Nambu, *Phys. Rev.* **117**, 648 (1960).
- [56] H. Bruus and K. Flensberg, *Many-Body Quantum Theory in Condensed Matter Physics - An Introduction* (Oxford University Press, New York, 2004).
- [57] G. Deutscher and P. de Gennes, in *Superconductivity*, edited by R. D. Parks, Vol. 2 (Marcel Dekker, Inc., New York, 1969), pp. 1005–34.
- [58] D. S. Falk, *Phys. Rev.* **132**, 1576 (1963).
- [59] M. Tinkham, *Introduction to Superconductivity* (Dover Publications, Inc., Mineola, NY, 2003).
- [60] T. Schäpers, *Superconductor/Semiconductor Junctions* (Springer-Verlag, Berlin, Heidelberg, 2001).
- [61] H. van Houten and C. Beenakker, *Phys. B: Condens. Matter* **175**, 187 (1991), analogies in Optics and Micro-Electronics.
- [62] A. Martin and J. F. Annett, *Superlattices Microstruct.* **25**, 1019 (1999).
- [63] H. Aizawa and K. Kuroki, *Phys. Rev. B* **97**, 104507 (2018).
- [64] S. Guéron, H. Pothier, N. O. Birge, D. Esteve, and M. H. Devoret, *Phys. Rev. Lett.* **77**, 3025 (1996).
- [65] K. D. Usadel, *Phys. Rev. Lett.* **25**, 507 (1970).
- [66] G. Eilenberger, *Z. Phys.* **214**, 195 (1968).
- [67] A. I. Larkin and Yu. N. Ovchinnikov, *Zh. Eksp. Teor. Fiz.* **55**, 2262 (1969) [*JETP* **28**, 1200 (1969)].
- [68] V. L. Ginzburg and L. D. Landau, *Zh. Eksp. Teor. Fiz.* **20**, 1064 (1950) *Collected Papers of L.D. Landau*, edited by D. ter Haar (Pergamon Press, Oxford, 1965), pp. 546–568.
- [69] L. P. Gor'kov, *Zh. Eksp. Teor. Fiz.* **36**, 1918 (1959) [*JETP* **9**, 1364 (1959)].
- [70] J. Ridderbos, M. Brauns, F. K. de Vries, J. Shen, A. Li, S. Kölling, M. A. Verheijen, A. Brinkman, W. G. van der Wiel, E. P. A. M. Bakkers, and F. A. Zwanenburg, *Nano Lett.* **20**, 122 (2020).
- [71] C. Reeg, D. Loss, and J. Klinovaja, *Phys. Rev. B* **96**, 125426 (2017).
- [72] W. S. Cole, S. Das Sarma, and T. D. Stanescu, *Phys. Rev. B* **92**, 174511 (2015).
- [73] J. Klinovaja and D. Loss, *Phys. Rev. B* **86**, 085408 (2012).
- [74] J. Osca and L. Serra, *Phys. Rev. B* **88**, 144512 (2013).
- [75] G. Livanas, N. Vanas, and G. Varelogiannis, *Condens. Matter* **6**, 44 (2021).
- [76] M. Alidoust, K. Halterman, and O. T. Valls, *Phys. Rev. B* **92**, 014508 (2015).
- [77] G.-Q. Zha, L. Covaci, F. M. Peeters, and S.-P. Zhou, *Phys. Rev. B* **91**, 214504 (2015).
- [78] C.-T. Wu, O. T. Valls, and K. Halterman, *Phys. Rev. B* **86**, 014523 (2012).
- [79] K. Halterman, O. T. Valls, and P. H. Barsic, *Phys. Rev. B* **77**, 174511 (2008).
- [80] K. Halterman, P. H. Barsic, and O. T. Valls, *Phys. Rev. Lett.* **99**, 127002 (2007).
- [81] Y. V. Fominov, A. A. Golubov, and M. Y. Kupriyanov, *JETP Lett.* **77**, 510 (2003).
- [82] H.-Y. Hui, P. M. R. Brydon, J. D. Sau, S. Tewari, and S. D. Sarma, *Sci. Rep.* **5**, 8880 (2015).
- [83] K. Halterman and M. Alidoust, *Phys. Rev. B* **98**, 134510 (2018).
- [84] K. Halterman and O. T. Valls, *Phys. Rev. B* **72**, 060514(R) (2005).
- [85] K. Halterman and O. T. Valls, *Physica C: Superconductivity* **397**, 151 (2003).
- [86] F. S. Bergeret, A. F. Volkov, and K. B. Efetov, *Phys. Rev. Lett.* **86**, 4096 (2001).
- [87] K. Halterman and O. T. Valls, *Phys. Rev. B* **65**, 014509 (2001).
- [88] G. Yang, C. Ciccarelli, and J. W. A. Robinson, *APL Mater.* **9**, 050703 (2021).
- [89] Y. N. Proshin, Y. A. Izyumov, and M. G. Khusainov, *Physica C: Superconductivity* **367**, 181 (2002).
- [90] K. Halterman and M. Alidoust, *Phys. Rev. B* **94**, 064503 (2016).
- [91] L. R. Tagirov, *Phys. Rev. Lett.* **83**, 2058 (1999).
- [92] M. Alidoust and K. Halterman, *Phys. Rev. B* **97**, 064517 (2018).
- [93] A. I. Buzdin, *Rev. Mod. Phys.* **77**, 935 (2005).
- [94] E. Anderson, Z. Bai, C. Bischof, S. Blackford, J. Demmel, J. Dongarra, J. Du Croz, A. Greenbaum, S. Hammarling, A. McKenney, and D. Sorensen, *LAPACK Users' Guide*, 3rd ed. (Society for Industrial and Applied Mathematics, Philadelphia, PA, 1999).
- [95] S. Arabas, D. Jarecka, A. Jaruga, and M. Fijałkowski, *Scientific Programming* **22**, 201 (2014).
- [96] J.-X. Zhu, *Bogoliubov de Gennes Methods and its Applications* (Springer, Berlin, 2016).
- [97] N. N. Bogoliubov, *Nuovo Cimento* **7**, 794 (1958).
- [98] C. R. Reeg and D. L. Maslov, *Phys. Rev. B* **94**, 020501(R) (2016).
- [99] C. Beenakker, *Quantum Dots: A Doorway to Nanoscale Physics* (Springer, Berlin, Heidelberg, 2005), pp. 131–174.
- [100] S. Vaitiekėnas, G. W. Winkler, B. van Heck, T. Karzig, M.-T. Deng, K. Flensberg, L. I. Glazman, C. Nayak, P. Krogstrup, R. M. Lutchyn, and C. M. Marcus, *Science* **367**, eaav3392 (2020).
- [101] F. Peñaranda, R. Aguado, P. San-Jose, and E. Prada, *Phys. Rev. Res.* **2**, 023171 (2020).
- [102] A. Kringhøj, G. W. Winkler, T. W. Larsen, D. Sabonis, O. Erlandsson, P. Krogstrup, B. van Heck, K. D. Petersson, and C. M. Marcus, *Phys. Rev. Lett.* **126**, 047701 (2021).
- [103] T. D. Stanescu and S. Das Sarma, *Phys. Rev. B* **106**, 085429 (2022).
- [104] T. Kiendl, F. von Oppen, and P. W. Brouwer, *Phys. Rev. B* **100**, 035426 (2019).
- [105] H. Zhang, D. E. Liu, M. Wimmer, and L. P. Kouwenhoven, *Nat. Commun.* **10**, 5128 (2019).
- [106] F. Maier, J. Klinovaja, and D. Loss, *Phys. Rev. B* **90**, 195421 (2014).

- [107] T. D. Stanescu and S. Tewari, *J. Phys.: Condens. Matter* **25**, 233201 (2013).
- [108] Ö. Gül, H. Zhang, J. D. S. Bommer, M. W. A. de Moor, D. Car, S. R. Plissard, E. P. A. M. Bakkers, A. Geresdi, K. Watanabe, T. Taniguchi, and L. P. Kouwenhoven, *Nat. Nanotechnol.* **13**, 192 (2018).
- [109] O. Millo and G. Koren, *Philos. Trans. R. Soc. London A* **376**, 20140143 (2018).
- [110] W. Ko, J. L. Lado, and P. Maksymovych, *Nano Lett.* **22**, 4042 (2022).
- [111] M. Hashisaka, T. Jonckheere, T. Akiho, S. Sasaki, J. Rech, T. Martin, and K. Muraki, *Nat. Commun.* **12**, 2794 (2021).
- [112] P. Chalsani, S. K. Upadhyay, O. Ozatay, and R. A. Buhrman, *Phys. Rev. B* **75**, 094417 (2007).
- [113] A. Gupta, L. Crétonon, B. Pannetier, and H. Courtois, *Pramana J. Phys.* **66**, 251 (2006).
- [114] N. A. Mortensen, K. Flensberg, and A.-P. Jauho, *Phys. Rev. B* **59**, 10176 (1999).
- [115] O. Šipr and B. L. Györfy, *J. Low Temp. Phys.* **106**, 315 (1997).
- [116] C. W. J. Beenakker, *Rev. Mod. Phys.* **69**, 731 (1997).
- [117] B. Béri, J. N. Kupferschmidt, C. W. J. Beenakker, and P. W. Brouwer, *Phys. Rev. B* **79**, 024517 (2009).
- [118] T. D. Stanescu and S. Das Sarma, *Phys. Rev. B* **96**, 014510 (2017).